5-1-2019

Numerical Analysis and Fluid Flow Modeling of Incompressible Navier-Stokes Equations

Tahj Hill
tahjhill@gmail.com

NUMERICAL ANALYSIS AND FLUID FLOW MODELING OF INCOMPRESSIBLE NAVIER-STOKES EQUATIONS

By

Tahj Hill

Bachelor of Science – Mathematical Sciences
University of Nevada, Las Vegas
2013

A thesis submitted in partial fulfillment
of the requirements for the

Master of Science – Mathematical Sciences

Department of Mathematical Sciences
College of Sciences
The Graduate College

University of Nevada, Las Vegas
May 2019

UNLV | GRADUATE COLLEGE

Thesis Approval

The Graduate College
The University of Nevada, Las Vegas

April 4, 2019

This thesis prepared by

Tahj Hill

entitled

Numerical Analysis and Fluid Flow Modeling of Incompressible Navier-Stokes Equations

is approved in partial fulfillment of the requirements for the degree of

Master of Science - Mathematical Sciences
Department of Mathematical Sciences

Monika Neda, Ph.D.
Examination Committee Chair

Kathryn Hausbeck Korgan, Ph.D.
Graduate College Dean

Zhonghai Ding, Ph.D.
Examination Committee Member

Xin Li, Ph.D.
Examination Committee Member

Dong-Chan Lee, Ph.D.
Graduate College Faculty Representative

ABSTRACT

NUMERICAL ANALYSIS AND FLUID FLOW MODELING OF INCOMPRESSIBLE NAVIER-STOKES EQUATIONS

by

Tahj Hill

Monika Neda, Examination Committee Chair
Professor of Mathematical Sciences
University of Nevada, Las Vegas

The Navier-Stokes equations (NSE) are an essential set of partial differential equations for governing the motion of fluids. In this paper, we will study the NSE for an incompressible flow, one which density $\rho = \rho_0$ is constant.

First, we will present the derivation of the NSE and discuss solutions and boundary conditions for the equations. We will then discuss the Reynolds number, a dimensionless number that is important in the observations of fluid flow patterns. We will study the NSE at various Reynolds numbers, and use the Reynolds number to write the NSE in a nondimensional form.

We will then derive energy and enstrophy balances for the NSE. At high Reynolds numbers, a fluid's velocity $\mathbf{u}$ has many small spatial scales, which become difficult to account for, especially in three-dimensional flow. We discuss the time relaxation model (TRM), which

aims to truncate these small scales while allowing the large scales to be accurately resolved, [25]. We will derive the energy and enstrophy balances for the TRM and show that the energy and enstrophy are the same as the NSE, but with enhanced dissipation terms.

Finally, we will derive a continuous finite element variational formulation for the TRM. Using FreeFEM++, we will run numerical results for the TRM for a specific benchmark problem.

TABLE OF CONTENTS

LIST OF FIGURES

LIST OF ALGORITHMS

CHAPTER 1

NAVIER-STOKES EQUATIONS

Introduction

The Navier-Stokes Equations (NSE) are an essential set of partial differential equations for governing the motion of fluids. Originally derived by Claude-Louis Navier in 1823, with a more rigorous derivation by George Gabriel Stokes in 1845, the NSE are based upon the application of the following important physical principles: Newton's law of viscosity, which relates shear stress in a fluid to the rate of distortion of fluid elements; the conservation of mass, which states the mass of an isolated system remains constant over time; and Newton's second law, Force = mass $\times$ acceleration [6].

For a region Ω and $0 < t \leq T$, the Navier-Stokes equations are defined as

$$\rho\left(\mathbf{u}_t + \mathbf{u} \cdot \nabla \mathbf{u}\right) - \mu \Delta \mathbf{u} + \nabla p = \mathbf{f}, \tag{1.1}$$

$$\nabla \cdot \mathbf{u} = 0, \tag{1.2}$$

where $\mathbf{u}(x,t)$ is the fluid velocity, μ is the dynamic viscosity, ρ is density, $p(x,t)$ is the fluid pressure, and $\mathbf{f}(x,t)$ is the body force. Equation (1.1) is known as the *Cauchy momentum equation*, which governs momentum transport, and equation (1.2) is known as the *mass con-*

tinuity equation, which describes the movement of mass through a continuous fluid, [12].

Today, the NSE are of importance because they are complete equations of motion for a viscous Newtonian fluid, one which obeys a general relationship between shear stress and velocity. Viscosity, the measure of a fluid's resistance to shear when in motion, decreases with increasing temperature in a liquid while increasing with decreasing temperature in a gas. The NSE describes the motion of fluids, such as air and water, from their laminar to turbulent flows. As velocity increases, the flow of a fluid will change from laminar, flowing in layers, to turbulent, having random fluctuations. As such, fluid velocity is a common variable in applications of the NSE, as well as density ρ, pressure p, external forces $\mathbf{f}$, and tensor stress $\overrightarrow{t}$, [3], [6]. Herein, we will study the NSE for an incompressible flow, one which density $\rho = \rho_0$ is constant.

Derivation of the Navier-Stokes Equations

The equations (1.1) and (1.2) are based on the conservation of momentum and conservation of mass, respectively. The mass continuity equation states that if mass is conserved, the rate of change of mass in a volume V is equal to the net mass flux across the boundary ∂V, [24]. The Cauchy momentum equation states that the rate of change of linear motion equals the net forces acting on a collection of fluid particles, or $Force = mass \times acceleration$, [24]. Below, we present the derivations of the two equations, beginning with the mass continuity equation.

Mass Continuity Equation

For a density ρ, the rate of change of mass is written as

$$\frac{\partial}{\partial t}\int_V \rho dx, \tag{1.3}$$

where $\frac{\partial}{\partial t}$ represents the rate of change and $\int_V \rho dx$ is the total mass.

Let $\mathbf{n}$ be the outward normal to ∂V and take $\mathbf{u}\cdot\mathbf{n} < 0$ to represent the inflow through ∂V. Then the net mass influx across the boundary is given by

$$-\int_{\partial V} (\rho\mathbf{u})\cdot\mathbf{n} d\sigma. \tag{1.4}$$

Since (1.3) and (1.4) are equal, the mass continuity equation is given by

$$\frac{\partial}{\partial t}\int_V \rho dx = -\int_{\partial V} (\rho\mathbf{u})\cdot\mathbf{n} d\sigma. \tag{1.5}$$

By the divergence theorem,

$$\int_{\partial V} (\rho\mathbf{u})\cdot\mathbf{n} d\sigma = \int_V \nabla\cdot(\rho\mathbf{u})\, dx.$$

Then (1.5) becomes

$$\int_V \frac{\partial\rho}{\partial t} = -\int_V \nabla\cdot(\rho\mathbf{u})\, dx,$$

which becomes

$$\int_V \frac{\partial \rho}{\partial t} + \nabla \cdot (\rho \mathbf{u})\, dx = 0. \tag{1.6}$$

Equation (1.6) holds for any arbitrary volume V. Thus, if all variables are continuous, it must also hold at a single point, [34]. Therefore, reducing V to a single point gives

$$\frac{\partial \rho}{\partial t} + \nabla \cdot (\rho \mathbf{u}) = 0. \tag{1.7}$$

If the fluid is incompressible, then density ρ is constant. Thus $\rho(x,t) \equiv \rho_0$ and the conservation of mass reduces to the *divergence-free condition*:

$$\nabla \cdot \mathbf{u} = 0, \tag{1.8}$$

as desired.

Cauchy Momentum Equation

Consider a fluid particle at position $\mathbf{x}$ and time t, and note that acceleration is the derivative of the velocity vector with respect to time. Since $\mathbf{u}$ depends only on time and position coordinates (i.e. $\mathbf{u} = \mathbf{u}(\mathbf{x}, t)$), we may apply the *material derivative*, defined as

$$\frac{D\mathbf{u}}{Dt} = \frac{\partial \mathbf{u}}{\partial t} + \sum_j u_j \frac{\partial u_i}{\partial x_j} = \mathbf{u}_t + \mathbf{u} \cdot \nabla \mathbf{u}.$$

Then the acceleration term reduces to

$$\frac{D\mathbf{u}}{Dt} = \mathbf{u}_t + (\mathbf{u} \cdot \nabla)\,\mathbf{u}. \tag{1.9}$$

Thus, for a volume V, $Force = mass \ \times \ acceleration$ gives

$$\int_V \rho\,(\mathbf{u}_t + \mathbf{u} \cdot \nabla \mathbf{u})\,dx = \mathbb{F}.$$

External forces, such as gravity, buoyancy, and electromagnetic forces, are collected in a body force term $\int_V \mathbf{f} dx$, while the net contribution of internal forces, such as pressure, is given by the *Cauchy stress tensor*, denoted $\overrightarrow{t}$. Thus, the net contribution of internal forces on V is $\int_S \overrightarrow{t}\, dS$, where $S = \partial V$. Therefore, $\mathbb{F}$ becomes

$$\int_V \rho\,(\mathbf{u}_t + \mathbf{u} \cdot \nabla \mathbf{u})\,dx = \int_V \mathbf{f} dx + \int_S \overrightarrow{t}\, dS. \tag{1.10}$$

Cauchy stress tensor $\overrightarrow{t}$ is a linear function of $\hat{n}$, the normal vector to the imaginary plane, [24]. Then there is a 3×3 matrix $\mathbf{\Pi}$ such that $\overrightarrow{t}(\hat{n}) = \hat{n} \cdot \mathbf{\Pi}$. Thus,

$$\begin{aligned}
\int_V \rho\,(\mathbf{u}_t + \mathbf{u} \cdot \nabla \mathbf{u})\,dx &= \int_V \overrightarrow{t}(\hat{n}) d\sigma + \int_V \mathbf{f} dx, \\
&= \int_{\partial V} n \cdot \mathbf{\Pi} d\sigma + \int_V \mathbf{f} dx, \\
&= \int_V (\nabla \cdot \mathbf{\Pi} + \mathbf{f}) dx.
\end{aligned}$$

As with (1.6), the previous equation holds for any arbitrary volume V. Therefore, if all

variables are continuous, it must also hold at a single point. Shrinking V to a point gives

$$\rho\left(\mathbf{u}_t + \mathbf{u}\cdot\nabla\mathbf{u}\right) = \nabla\cdot\mathbf{\Pi} + \mathbf{f}. \tag{1.11}$$

The stress tensor $\mathbf{\Pi}$ consists of a pressure force and a non-pressure part, known as the viscous stress tensor $\mathbf{V}$, [24]. For an incompressible flow, define the dynamic pressure as $p := \frac{1}{3}\left(\Pi_{11} + \Pi_{22} + \Pi_{33}\right)$. Then the pressure force is

$$\text{pressure force} = -p\mathbf{I}\hat{n},$$

where $\mathbf{I}$ is the identity matrix. Thus, the stress tensor is defined as

$$\mathbf{\Pi} = -p\mathbf{I} + \mathbf{V}.$$

Or, in matrix form,

$$\mathbf{\Pi} = \begin{pmatrix} \Pi_{11} & \Pi_{12} & \Pi_{13} \\ \Pi_{21} & \Pi_{22} & \Pi_{23} \\ \Pi_{31} & \Pi_{32} & \Pi_{33} \end{pmatrix} = -\begin{pmatrix} p & 0 & 0 \\ 0 & p & 0 \\ 0 & 0 & p \end{pmatrix} + \begin{pmatrix} \Pi_{11}+p & \Pi_{12} & \Pi_{13} \\ \Pi_{21} & \Pi_{22}+p & \Pi_{23} \\ \Pi_{31} & \Pi_{32} & \Pi_{33}+p \end{pmatrix}.$$

Let $\mathbf{D}$ be the deformation tensor, defined as $\mathbf{D} = \nabla\mathbf{u} + \nabla\mathbf{u}^T$. Since the fluid is a Newtonian fluid, it satisfies the assumption that $\mathbf{V} = \mu\mathbf{D}$, [24]. Therefore, plugging in values to (1.11),

$$\rho\left(\mathbf{u}_t + \mathbf{u}\cdot\nabla\mathbf{u}\right) + \nabla p - \nabla\cdot\left(\mu\mathbf{D}(u)\right) = \mathbf{f}. \tag{1.12}$$

It can be shown that $\mu\nabla \cdot \mathbf{D}(\mathbf{u}) = \mu\Delta\mathbf{u}$, [24]. Dividing (1.12) by ρ, the equation becomes

$$\mathbf{u}_t + \mathbf{u} \cdot \nabla\mathbf{u} + \nabla p + \nu\Delta\mathbf{u} = \mathbf{f}, \tag{1.13}$$

where the pressure p is redefined $p = p/\rho_0$ and $\nu = \mu/\rho_0$, known as the kinematic viscosity, [24].

Solutions and Boundary Conditions of the NSE

Term $\mathbf{u} \cdot \nabla\mathbf{u}$ in the momentum equation is called the *inertial term*. It is the only nonlinear term in the Navier-Stokes equations. Unlike many equations in mathematical physics, the nonlinearity comes from the mathematical aspects of the problem rather than the physical attributes of the system, [19]. Due to the nonlinearity of the inertial term, the question of existence and uniqueness must be raised for the given boundary conditions. For the given physics, it is not guaranteed that a satisfactory solution exists. Thus, boundary conditions and function spaces must be considered, [19].

Two possible types of boundary conditions considered for the NSE are the no-slip boundary conditions, where the velocity is zero on the boundary, and space-periodic boundary conditions, which are used to study idealized flows far away from real boundaries. No-slip boundary conditions are used when a fluid fills a smooth, bounded domain with a rigid boundary, and they are more physically practical than space-periodic conditions. Space-periodic conditions, while not as physically practical, are useful for idealized models of certain flows, [19].

In solving the existence and uniqueness of the NSE, two types of solutions are considered: strong solutions and weak solutions. In two dimensions the weak solutions are actually strong solutions, they are unique, and they exist for all time. It is more complex in the three-dimensional case, however. Weak solutions are known to exist for all time, but are not known to be unique. Conversely, strong solutions are known to be unique and to exist on a certain finite time interval, but it is not known if they exist for all time, [19].

The mathematical gap between existence and uniqueness of the weak solutions of the three-dimensional NSE is the basis of much of the study of the equations. Since all practical fluid flows arise in the three-dimensional case, it is unknown if the NSE are a complete description of fluid flows. Furthermore, it is unclear if this gap is a property of real fluids or if there exists an inadequacy in the model, [19], [24]. This open problem for the three-dimensional case is known as the *fundamental problem* in the mathematical analysis of the NSE, and it is one of the million-dollar Clay prize problems, [24].

CHAPTER 2

REYNOLDS NUMBER AND TURBULENCE

Introduction

A major problem in early fluid mechanics was understanding flow patterns in pipes. In a pipe, the flow may be fully laminar, fully turbulent, or have turbulent regions, known as *turbulent slugs*, separated by laminar regions. The issue arose in how to use these observations to make predictions about turbulent flow occurring for different flow rates, pipe diameters, temperatures, and liquids, [24]. These predictions must also be made without actually observing the flow, for in many cases, direct observation is not possible, [26].

The character of flow in a round pipe is dependent on several variables: fluid density ρ, fluid viscosity μ, reference speed V and reference length L, [24]. Using these variables, as well as the concept of dimensional analysis, Osborne Reynolds demonstrated that flow patterns can be predicted if the magnitude of a dimensionless number is known, [26]. This number is known as the *Reynolds number*, and it is important in the observations of fluid flow patterns.

For fluid density ρ, reference length L, reference velocity U, and fluid viscosity μ, the Reynolds number is defined as

$$\mathrm{Re} := \frac{\rho U L}{\mu}. \tag{2.1}$$

Using standard SI units for example, it can be shown that the Reynolds number is dimensionless, [26]:

$$\begin{aligned} \mathrm{Re} &= \frac{\rho V L}{\mu} = \rho \times U \times L \times \frac{1}{\mu}, \\ &= \frac{\mathrm{kg}}{\mathrm{m}^3} \times \frac{\mathrm{m}}{\mathrm{s}} \times \mathrm{m} \times \frac{\mathrm{m} \cdot \mathrm{s}}{\mathrm{kg}}. \end{aligned}$$

Since all the units cancel, Re is dimensionless. It is still important, however, that all terms be consistent in units to obtain the correct numerical value, [26].

The Reynolds number represents the ratio of inertial forces to viscous forces. If Re is close to 0, the viscous forces dominate the inertial forces. An example of such is one of a highly viscous fluid moving slowly. For Re large, however, the viscous forces may be neglected, as in the flows of gases. The Reynolds number occurs in all flow settings, and is particularly useful in determining the pattern of fluid flow, as it can be used to determine whether a flow is laminar or turbulent, [24].

Fluid flows with a high Reynolds number are turbulent and those with lower numbers are laminar. In practical applications, a flow is assumed to be laminar if the Reynolds number is below 2000, and a flow is assumed to be turbulent if the Reynolds number is above 4000. Between 2000 and 4000, there is a region of uncertainty, called the *critical region*, where it is impossible to determine the behavior of the flow. In most applications, the flow is either in the well within the turbulent range or well within the laminar range. Thus, the critical region does not cause any difficulty, [26].

Nondimensionalization of the NSE

In the study of the NSE, it is advantageous to use a *nondimensional* form of the equations, in which we define dimensionless variables to replace the independent and dependent variables of the problem. This will allow us to study the equations in a general form, rather than for one distinct set of parameter values, [22]. Furthermore, it becomes easier to solve the NSE numerically in this form, as the information of the characteristics of a process can be stored in a few dimensionless parameters, rather than many dimensional ones, and it eliminates confusion about which units to store the dimensional parameters in, [10].

Consider the Cauchy momentum equation (1.1). Introduce dimensionless variables by expressing $t, \mathbf{u}, \mathbf{x}, p$ as fractions of the reference parameters L and U, as well as reference body acceleration G, i.e.

$$\hat{u}_i = \frac{u_i}{U}, \quad \hat{x}_k = \frac{x_k}{L}, \quad \hat{t} = \frac{U}{L}t, \quad \hat{p} = \frac{p}{\rho U^2}, \quad \hat{f} = \frac{f}{G}. \tag{2.2}$$

Note that

$$\frac{\partial}{\partial \hat{x}_k}\hat{u}_i = \frac{\partial}{\partial \hat{x}_k}\frac{u_i}{U} = \frac{1}{U}\frac{\partial}{\partial \hat{x}_k}u_i = \frac{L}{U}\frac{\partial}{\partial x_k}u_i.$$

Therefore,

$$\frac{\partial}{\partial x_k}u_i = \frac{U}{L}\frac{\partial}{\partial \hat{x}_k}\hat{u}_i.$$

We then nondimensionalize the NSE as follows. We use the two-dimensional case as three

dimensions are proved similarly. Take

$$\mathbf{u}_t = \frac{\partial}{\partial t}\mathbf{u} = \frac{\partial}{\partial t}\begin{pmatrix} \frac{\partial}{\partial t}u_1 \\ \\ \frac{\partial}{\partial t}u_2 \end{pmatrix} = \begin{pmatrix} \frac{\partial}{\partial t}U\hat{u}_1 \\ \\ \frac{\partial}{\partial t}U\hat{u}_2 \end{pmatrix} = \begin{pmatrix} U\frac{\partial}{\partial t}\hat{u}_1 \\ \\ U\frac{\partial}{\partial t}\hat{u}_2 \end{pmatrix} = U\begin{pmatrix} \frac{U}{L}\frac{\partial}{\partial \hat{t}}\hat{u}_1 \\ \\ \frac{U}{L}\frac{\partial}{\partial \hat{t}}\hat{u}_2 \end{pmatrix} = \frac{U^2}{L}\hat{\mathbf{u}}_{\hat{t}},$$

$$\mathbf{u}\cdot\nabla\mathbf{u} = \begin{pmatrix} u_1 \\ \\ u_2 \end{pmatrix}\cdot\begin{pmatrix} \frac{\partial}{\partial x}u_1 & \frac{\partial}{\partial x}u_2 \\ \\ \frac{\partial}{\partial y}u_1 & \frac{\partial}{\partial y}u_2 \end{pmatrix} = U\begin{pmatrix} \hat{u}_1 \\ \\ \hat{u}_2 \end{pmatrix}\cdot\frac{U}{L}\begin{pmatrix} \frac{\partial}{\partial \hat{x}}\hat{u}_1 & \frac{\partial}{\partial \hat{x}}\hat{u}_2 \\ \\ \frac{\partial}{\partial \hat{y}}\hat{u}_1 & \frac{\partial}{\partial \hat{y}}\hat{u}_2 \end{pmatrix} = \frac{U^2}{L}\hat{\mathbf{u}}\cdot\hat{\nabla}\hat{\mathbf{u}},$$

$$\Delta\mathbf{u} = \begin{pmatrix} \Delta u_1 \\ \\ \Delta u_2 \end{pmatrix} = \begin{pmatrix} \frac{\partial}{\partial x}\left(\frac{\partial}{\partial x}u_1\right) + \frac{\partial}{\partial y}\left(\frac{\partial}{\partial y}u_1\right) \\ \\ \frac{\partial}{\partial x}\left(\frac{\partial}{\partial x}u_2\right) + \frac{\partial}{\partial y}\left(\frac{\partial}{\partial y}u_2\right) \end{pmatrix} = \begin{pmatrix} \frac{U}{L^2}\left(\hat{\Delta}\hat{u}_1\right) \\ \\ \frac{U}{L^2}\left(\hat{\Delta}\hat{u}_2\right) \end{pmatrix} = \frac{U}{L^2}\hat{\Delta}\hat{\mathbf{u}},$$

$$\nabla p = \begin{pmatrix} \frac{\partial}{\partial x}p \\ \\ \frac{\partial}{\partial y}p \end{pmatrix} = \frac{\rho U^2}{L}\begin{pmatrix} \frac{\partial}{\partial \hat{x}}\hat{p} \\ \\ \frac{\partial}{\partial \hat{y}}\hat{p} \end{pmatrix} = \frac{\rho U^2}{L}\hat{\nabla}\hat{p}.$$

Then the Cauchy momentum equation becomes

$$\frac{U^2}{L}\hat{\mathbf{u}}_{\hat{t}} + \frac{U^2}{L}\hat{\mathbf{u}}\cdot\hat{\nabla}\hat{\mathbf{u}} - \nu\frac{U}{L^2}\hat{\Delta}\hat{\mathbf{u}} + \frac{1}{\rho}\frac{\rho U^2}{L}\hat{\nabla}\hat{p} = G\hat{f},$$

and the mass continuity equation becomes

$$\nabla\cdot\mathbf{u} = \frac{\partial u_1}{\partial x_1} + \frac{\partial u_2}{\partial x_2} = \frac{\partial U\hat{u}_1}{\partial x_1} + \frac{\partial U\hat{u}_2}{\partial x_2} = U\left(\frac{\partial \hat{u}_1}{\partial x_1} + \frac{\partial \hat{u}_2}{\partial x_2}\right) = U\left(\hat{\nabla}\cdot\hat{\mathbf{u}}\right).$$

Since the continuity equation is equal to zero, we may divide both sides by U to get

$$\hat{\nabla}\cdot\hat{\mathbf{u}} = 0.$$

Next, dividing both sides of the momentum equation by $\frac{U^2}{L}$ gives

$$\hat{\mathbf{u}}_{\hat{t}} + \hat{\mathbf{u}} \cdot \hat{\nabla}\hat{\mathbf{u}} - \nu \frac{1}{UL}\hat{\Delta}\hat{\mathbf{u}} + \frac{\rho U^2}{L}\hat{\nabla}\hat{p} = \left(\frac{LG}{U^2}\right)\hat{f}.$$

Finally, dropping the superscripts for simplicity, the nondimensional Navier-Stokes Equations are

$$\mathbf{u}_t + \mathbf{u} \cdot \nabla\mathbf{u} - \mathrm{Re}^{-1}\Delta\mathbf{u} + \nabla p = \frac{1}{\mathrm{Fr}^2}\mathbf{f};$$
$$\nabla \cdot \mathbf{u} = 0.$$

This new system depends only on two parameters: the Reynolds's number Re and the *Froude number*, $\mathrm{Fr} = \frac{U}{\sqrt{GL}}$, which measures the influence of the gravitational field on the inertial flow, [2], [10].

When nondimensionalizing the NSE, it is necessary to determine which factor we are most interested in studying. For purposes of this paper, we wish to study the effects of various Reynolds numbers on the NSE. Thus, we will assume the Froude number is equal to 1, i.e. there is a perfect balance of the gravitational and inertial forces, to better observe the influence of the Reynolds number later, [2], [10]. Therefore, the final nondimensional NSE is given by

$$\mathbf{u}_t + \mathbf{u} \cdot \nabla\mathbf{u} - \mathrm{Re}^{-1}\Delta\mathbf{u} + \nabla p = \mathbf{f}; \tag{2.3}$$
$$\nabla \cdot \mathbf{u} = 0. \tag{2.4}$$

Throughout the remainder of this paper, we will refer to (2.3) and (2.4) when discussing the NSE.

Stokes Flow

In many studies of fluid flow, it is of interest to consider the case when Re is small, i.e. $\mathrm{Re} \ll 1$. This is attained by dealing with a very viscous liquid, or flows with very small velocity, also known as creeping flows. These special cases are referred to as *Stokes flow*, [9].

Since Re is small, the viscous forces are dominant. Therefore, we may drop the $\mathbf{u}_t$ and $\mathbf{u} \cdot \nabla \mathbf{u}$ terms from (2.3)-(2.4), thus linearizing the system, [9]. The Stokes equation is then

$$-\Delta \mathbf{u} + \nabla p = \mathbf{f}; \tag{2.5}$$

$$\nabla \cdot \mathbf{u} = 0. \tag{2.6}$$

Turbulent Flow and the Navier-Stokes Equations

Compared to laminar flow, turbulent flows are more prevalent in applications, but less easily seen, [29]. Their structures are far more complicated than those of laminar flows, making the study of turbulent flow meaningful, yet difficult, [24]. Three key reasons for studying turbulent flows include their prevalence in applications, the transport of mixing and matter by turbulent flows, and the effects of turbulence on these processes.

Turbulent flows transport and mix fluid much more effectively than comparable laminar flows. This is important in many applications because when different fluids are brought in to mix, it is desirable for the mixture to take place as quickly as possible, [29]. Because shear stress is larger in turbulent flows, they are effective at "mixing" the momentum of a fluid. For example, rates of heat and mass transfer at liquid-gas and solid-fluid interfaces are more enhanced in turbulent flows.

In the study of turbulence, there is a need to distinguish between small- and large-scale motion of turbulent flows. At high Reynolds numbers, there is a separation of scales. The behavior of large-scale motions is influenced by the geometry of the flow and controls the transport and mixing of fluids. Conversely, the behavior of small-scale motion is mostly determined by the viscosity and the rate at which they receive energy from the large scales. Thus, the small-scale motion is independent of the flow geometry, [29].

In turbulent flow, there exists a critical length scale of eddies called the *Kolmogorov microscale*. Large eddies below this critical size are dominated by viscous forces and die very quickly because of them. The Kolmogorov microscale is defined as $O(\mathrm{Re}^{-\frac{3}{4}})$ in three dimensions and $O(\mathrm{Re}^{-\frac{1}{2}})$ for two-dimensional turbulence, [24].

Turbulent flow consists of an energy cascade of three-dimensional eddies of various sizes. Solutions of the Navier-Stokes Equations exhibit this energy cascade due to certain fundamental properties they contain. First, if kinematic viscosity $\nu = 0$, then the kinetic energy of the flow is conserved. Second, the nonlinearity of the NSE conserves energy globally, but

it breaks large eddies into smaller ones, thus transferring energy to smaller scales, [24].

If $\nu > 0$, then the viscous terms dissipate energy from the flow globally, [24]. Except on very small scales of motion, the energy dissipation due to the viscous terms is negligible for Re large. Finally, the forces driving the flow persistently input energy into the largest scales of motion, [24].

Essentially, these properties of the NSE give information that energy is put into the largest scales of the flow. There is an intermediate range where the nonlinearity of the NSE drives the energy into smaller scales. At sufficiently small scales, however, dissipation is not negligible, and the energy in the smallest scales decays to zero exponentially fast, [24].

CHAPTER 3

ENERGY AND ENSTROPHY OF THE NAVIER-STOKES EQUATIONS

Energy Balance

Consider the Navier-Stokes Equations (2.3)–(2.4). Multiplying by $\mathbf{u}$ and integrating along the region Ω, we obtain

$$\begin{aligned}
\int_\Omega \left[\mathbf{u}_t \cdot \mathbf{u} + \mathbf{u} \cdot \mathbf{u}\nabla\mathbf{u} - \mathbf{u}\mathrm{Re}^{-1}\Delta\mathbf{u} + \mathbf{u}\nabla p\right]\, d\Omega &= \int_\Omega \mathbf{f} \cdot \mathbf{u}\, d\Omega, \\
\int_\Omega \mathbf{u}_t \cdot \mathbf{u}\, d\Omega + \int_\Omega \mathbf{u}\nabla\mathbf{u} \cdot \mathbf{u}\, d\Omega - \mathrm{Re}^{-1}\int_\Omega \mathbf{u}\Delta\mathbf{u}\, d\Omega + \int_\Omega \mathbf{u}\nabla p\, d\Omega &= \int_\Omega \mathbf{f} \cdot \mathbf{u}\, d\Omega, \\
\frac{1}{2}\frac{d}{dt}\int_\Omega \mathbf{u} \cdot \mathbf{u}\, d\Omega + \int_\Omega \mathbf{u}\nabla\mathbf{u} \cdot \mathbf{u}\, d\Omega - \mathrm{Re}^{-1}\int_\Omega \mathbf{u}\Delta\mathbf{u}\, d\Omega + \int_\Omega \mathbf{u}\nabla p\, d\Omega &= \int_\Omega \mathbf{f} \cdot \mathbf{u}\, d\Omega.
\end{aligned}$$

Let $\sigma = \partial\Omega$ and assume $\mathbf{u} = \mathbf{0}$ on the boundary. Then,

$$\begin{aligned}
&\frac{1}{2}\frac{d}{dt}\int_\Omega \mathbf{u} \cdot \mathbf{u}\, d\Omega = \frac{1}{2}\left\|\mathbf{u}\right\|^2, \\
&\int_\Omega \mathbf{u}\nabla\mathbf{u} \cdot \mathbf{u}\, d\Omega = (\mathbf{u}\nabla\mathbf{u}, \mathbf{u}) = 0, \\
&\mathrm{Re}^{-1}\int_\Omega \mathbf{u}\Delta\mathbf{u} = -\mathrm{Re}^{-1}\int_\Omega \nabla\mathbf{u}\nabla\mathbf{u}\, d\Omega + \mathrm{Re}^{-1}\int_\sigma \nabla\mathbf{u} \cdot n \cdot \mathbf{u} d\sigma = \mathrm{Re}^{-1}\left\|\Delta\mathbf{u}\right\|^2, \\
&\int_\Omega \mathbf{u}\nabla p\, d\Omega = -\int_\Omega p\Delta\mathbf{u}\, d\Omega + \int_\sigma p\mathbf{u} \cdot n d\sigma = 0.
\end{aligned}$$

Therefore,

$$\frac{1}{2}\frac{d}{dt}\left\|\mathbf{u}\right\|^2 + \mathrm{Re}^{-1}\left\|\nabla\mathbf{u}\right\|^2 = (\mathbf{f},\mathbf{u}). \tag{3.1}$$

Integrating (3.1) with respect to time,

$$\int_0^T \frac{1}{2}\frac{d}{dt}\left\|\mathbf{u}\right\|^2\,dt + \int_0^T \mathrm{Re}^{-1}\left\|\nabla\mathbf{u}\right\|^2\,dt = \int_0^T (\mathbf{f},\mathbf{u})\,dt.$$

This equation becomes

$$\frac{1}{2}\left\|\mathbf{u}(T)\right\|^2 - \frac{1}{2}\left\|\mathbf{u}(0)\right\|^2 + \mathrm{Re}^{-1}\int_0^T \left\|\nabla\mathbf{u}\right\|^2\,dt = \int_0^T (\mathbf{f},\mathbf{u})\,dt, \tag{3.2}$$

where $\frac{1}{2}\left\|\mathbf{u}(T)\right\|^2$ is the kinetic energy at time T, $\frac{1}{2}\left\|\mathbf{u}(0)\right\|^2$ is the initial kinetic energy, $\mathrm{Re}^{-1}\int_0^T \left\|\nabla\mathbf{u}\right\|^2\,dt$ is the total energy dissipated over $[0,T]$, and $\int_0^T (\mathbf{f},\mathbf{u})\,dt$ is the total power input over $[0,T]$.

Enstrophy

Vorticity is defined as the curl of the velocity vector, and rises due to the frictional or viscous effects of a fluid. Mathematically, it is defined as

$$\omega = \nabla\times\mathbf{u}. \tag{3.3}$$

Enstrophy, then, is the integral of the square of the vorticity vector, [19]:

$$\mathit{Enstrophy}(t) := \frac{1}{2}\left\|\nabla\times\mathbf{u}\right\|^2 = \frac{1}{2}\int_\Omega \left|\nabla\times\mathbf{u}\right|^2 d\Omega = \frac{1}{2}\left(\nabla\times\mathbf{u},\nabla\times\mathbf{u}\right). \tag{3.4}$$

Enstrophy, and by extension vorticity, play an important role in the solutions to the NSE. For the strong solutions, the enstrophy is finite at all times, while for the weak solutions, the enstrophy may become infinite at some points in time, [19].

The transfer of enstrophy is directly related to the transfer of energy in two-dimensional turbulence. Above the range where energy is injected into the system, it goes from lower modes to higher modes, and in the range below the injection of energy, it goes from higher modes to lower modes. Enstrophy has a similar transfer: lower to higher in the range above the injection of energy, and higher to lower in the range below it. Within a certain range above the injection of energy, there is a higher transfer of enstrophy, causing a direct enstrophy cascade. Below the range, there is an inverse energy cascade, [19].

In this direct enstrophy cascade, the velocity field is separated into parts. These small parts contain eddies, or components of the wave flow, within a small range of length scales. Within a certain range of above the injection of energy, energy is transferred to smaller length scales, and therefore negligible dissipation. This similarity between energy and enstrophy in two dimensions is because in two dimensions, the vorticity has one component in the direction normal to the flow, which causes many constraints on the dynamics of the turbulence. As such, fluid flow in two dimensions must conserve enstrophy as well as energy, and the enstrophy and energy cascades may not exist on the same portions of a domain, [19].

Derivation of the Enstrophy Balance

Multiplying the Navier-Stokes Equations (2.3)–(2.4) by $\Delta\mathbf{u}$, we obtain

$$\mathbf{u}_t \cdot \Delta\mathbf{u} + \mathbf{u} \cdot \nabla\mathbf{u} \cdot \Delta\mathbf{u} - \mathrm{Re}^{-1}\Delta\mathbf{u} \cdot \Delta\mathbf{u} + \nabla p \cdot \Delta\mathbf{u} = \mathbf{f} \cdot \Delta\mathbf{u}.$$

Recall that $(\mathbf{u}, \mathbf{v}) = \int_\Omega \mathbf{u} \cdot \mathbf{v}\, d\Omega$. Integrating over domain Ω, we obtain

$$\int_\Omega \mathbf{u}_t \cdot \Delta\mathbf{u}\, d\Omega + \int_\Omega \mathbf{u} \cdot \nabla\mathbf{u} \cdot \Delta\mathbf{u}\, d\Omega - \int_\Omega \mathrm{Re}^{-1}\Delta\mathbf{u} \cdot \Delta\mathbf{u}\, d\Omega + \int_\Omega \nabla p \cdot \Delta\mathbf{u}\, d\Omega, \tag{3.5}$$

where

$$\begin{aligned}
\int_\Omega \mathbf{u}_t \cdot \Delta\mathbf{u}\, d\Omega &= -\int_\Omega (\nabla \times \mathbf{u}_t)(\nabla \times \mathbf{u})\, d\Omega, \\
&= -\frac{1}{2}\frac{d}{dt}\int_\Omega (\nabla \times \mathbf{u})(\nabla \times \mathbf{u})\, d\Omega, \\
&= -\frac{1}{2}\frac{d}{dt}\int_\Omega |\nabla \times \mathbf{u}|^2\, d\Omega, \\
&= -\frac{1}{2}\frac{d}{dt}\|\nabla \times \mathbf{u}\|^2 .
\end{aligned}$$

We also have

$$\begin{aligned}
&\int_\Omega \mathbf{u} \cdot \nabla\mathbf{u} \cdot \Delta\mathbf{u}\, d\Omega = (\mathbf{u}\nabla\mathbf{u}, \Delta\mathbf{u}) = 0, \\
&-\int_\Omega \mathrm{Re}^{-1}\Delta\mathbf{u} \cdot \Delta\mathbf{u}\, d\Omega = -\mathrm{Re}^{-1}\int_\Omega \Delta\mathbf{u} \cdot \Delta\mathbf{u}\, d\Omega = -\mathrm{Re}^{-1}\|\Delta\mathbf{u}\|^2, \\
&\int_\Omega \nabla p \Delta\mathbf{u}\, d\Omega = (\nabla p, \Delta\mathbf{u}) = \int_\Omega (\nabla \times \nabla p) \cdot (\nabla \times \mathbf{u})\, d\Omega = 0.
\end{aligned}$$

Let $\mathbf{f} = \mathbf{0}$, so that the right hand side is zero. Then we have

$$-\frac{1}{2}\frac{d}{dt}\left\|\nabla \times \mathbf{u}\right\|^2 - \mathrm{Re}^{-1}\left\|\Delta \mathbf{u}\right\|^2 = 0. \tag{3.6}$$

Multiplying by -1, we have

$$\frac{1}{2}\frac{d}{dt}\left\|\nabla \times \mathbf{u}\right\|^2 + \mathrm{Re}^{-1}\left\|\Delta \mathbf{u}\right\|^2 = 0.$$

Integrating with respect to time, we obtain

$$\int_0^T \left[\frac{1}{2}\frac{d}{dt}\left\|\nabla \times \mathbf{u}\right\|^2 + \mathrm{Re}^{-1}\left\|\Delta \mathbf{u}\right\|^2\right] dt = 0.$$

By the Fundamental Theorem of Calculus, this becomes

$$\frac{1}{2}\left\|\nabla \times \mathbf{u}(T)\right\|^2 - \frac{1}{2}\left\|\nabla \times \mathbf{u}(0)\right\|^2 + \mathrm{Re}^{-1}\int_0^T \left\|\Delta \mathbf{u}\right\|^2 dt = 0, \tag{3.7}$$

or

$$\frac{1}{2}\left\|\nabla \times \mathbf{u}(T)\right\|^2 + \mathrm{Re}^{-1}\int_0^T \left\|\Delta \mathbf{u}\right\|^2 dt = \frac{1}{2}\left\|\nabla \times \mathbf{u}(0)\right\|^2, \tag{3.8}$$

where $\mathrm{Re}^{-1}\displaystyle\int_0^T \left\|\Delta \mathbf{u}\right\|^2 dt$ is the enstrophy dissipation. Observe that enstrophy at time T is conserved in the absence of viscosity.

CHAPTER 4

TIME RELAXATION MODEL

Introduction

At high Reynolds numbers, fluid velocity **u** has many small spatial scales, which become difficult to account for, especially in three-dimensional flow. As such, the standard NSE becomes less computationally feasible because a very fine mesh is needed so that the computer can capture the small scales, [16], [17]. However, this runs the risk of altering the largest structures of the flow, which contain most of the flow's energy and are responsible for most of the mixing and flow's momentum transport, [25].

To reconcile this problem, many mathematical models have been developed and studied in computational fluid dynamics. One of the simplest and most widely applicable such models is the time relaxation model (TRM). Introduced by Stolz, Adams and Kleiser in [32], [33], the TRM aims to truncate the small scales in a solution, allowing the large scales to be accurately resolved without the computational and economic burden of resolving the smallest, [25].

From the Navier Stokes Equation (2.3)–(2.4), we obtain the *Time Relaxation Model*:

$$\mathbf{u}_t + \mathbf{u} \cdot \nabla \mathbf{u} - \mathrm{Re}^{-1} \Delta \mathbf{u} + \nabla p + \chi(\mathbf{u} - \bar{\mathbf{u}}) = \mathbf{f}, \tag{4.1}$$

$$\nabla \cdot \mathbf{u} = 0, \tag{4.2}$$

where χ is a scalar constant known as the relaxation parameter, and $\bar{\mathbf{u}}$ is the solution of the partial differential equation

$$-\delta^2 \Delta \bar{\mathbf{u}} + \bar{\mathbf{u}} = \mathbf{u}, \tag{4.3}$$

where δ is constant (filter width). For δ large, $\bar{\mathbf{u}}$ is smooth. For δ small, $\bar{\mathbf{u}}$ is close to $\mathbf{u}$.

Note that $\chi > 0$ and has units of $1/time$. The term $\chi(\mathbf{u} - \bar{\mathbf{u}})$ aims to drive the unresolved scales to zero exponentially fast, [17]. To use the time relaxation, the parameter χ must be specified and scaled appropriately with respect to other parameters in the problem, [25].

Energy Balance for the Time Relaxation Model

The solution of the time relaxation model is $\mathbf{u}$ and p such that they satisfy the system of partial differential equations (4.1)–(4.3). Assume $\mathbf{u} = \mathbf{0}$ on the boundary $\sigma = \partial\Omega$ and assume no body force $\mathbf{f} = \mathbf{0}$. The energy remains the same in the absence of body force, and the system changes if $\mathbf{f} \neq \mathbf{0}$ and/or if $\nu \neq 0$, where $\nu \approx \mathrm{Re}^{-1}$.

Multiplying (4.1) by $\mathbf{u}$, and integrating in space and time, we obtain

$$\int_\Omega \left[\mathbf{u}_t \cdot \mathbf{u} + \mathbf{u}(\mathbf{u}\cdot\nabla\mathbf{u}) - \mathbf{u}\cdot \mathrm{Re}^{-1}\Delta\mathbf{u} + \mathbf{u}\cdot\nabla p + \mathbf{u}\cdot\chi(\mathbf{u}-\bar{\mathbf{u}})\right]\, d\Omega = \int_\Omega \mathbf{f}\cdot\mathbf{u}\, d\Omega,$$

which becomes

$$\begin{aligned}\int_\Omega \mathbf{u}_t\cdot\mathbf{u}\, d\Omega + \int_\Omega \mathbf{u}\cdot\nabla\mathbf{u}\cdot\mathbf{u}\, d\Omega - \mathrm{Re}^{-1}\int_\Omega \mathbf{u}\cdot\Delta\mathbf{u}\, d\Omega \\ + \int_\Omega \mathbf{u}\cdot\nabla p\, d\Omega + \int_\Omega \mathbf{u}\cdot\chi(\mathbf{u}-\bar{\mathbf{u}})\, d\Omega = \int_\Omega \mathbf{f}\cdot\mathbf{u}\, d\Omega.\end{aligned}$$

Since $\mathbf{f}=\mathbf{0}$, the right hand side equals zero. Thus, we have

$$\int_\Omega \nabla p\cdot\mathbf{u}\, d\Omega = -\int_\Omega p(\nabla\cdot\mathbf{u})\, d\Omega + \int_\sigma p\cdot\mathbf{n}\cdot\mathbf{u} d\sigma = -\int_\Omega p(\nabla\cdot\mathbf{u})\, d\Omega = 0,$$

by (4.2). Take

$$\int_\Omega (\mathbf{u}\cdot\nabla\mathbf{u})\mathbf{u}\, d\Omega = 0.$$

Then

$$\begin{aligned}\int_\Omega \mathbf{u}\cdot\Delta\mathbf{u}\, d\Omega &= -\int_\Omega \nabla\mathbf{u}\cdot\nabla\mathbf{u}\, d\Omega + \int_\sigma \nabla\mathbf{u}\cdot\mathbf{n}\cdot\mathbf{u} d\sigma, \\ &= -\int_\Omega \nabla\mathbf{u}\cdot\nabla\mathbf{u}\, d\Omega, \\ &= \int_\Omega |\nabla\mathbf{u}|^2\, d\Omega, \\ &= \|\nabla\mathbf{u}\|^2.\end{aligned}$$

So we have

$$\int_\Omega \mathbf{u}_t \cdot \mathbf{u}\, d\Omega + \mathrm{Re}^{-1} \|\nabla \mathbf{u}\|^2 + \chi \int_\Omega (\mathbf{u} - \bar{\mathbf{u}})\mathbf{u}\, d\Omega = 0,$$
$$\frac{1}{2}\frac{d}{dt}\int_\Omega \mathbf{u} \cdot \mathbf{u}\, d\Omega + \mathrm{Re}^{-1} \|\nabla \mathbf{u}\|^2 + \chi \int_\Omega (\mathbf{u} - \bar{\mathbf{u}})\mathbf{u}\, d\Omega = 0,$$
$$\frac{1}{2}\frac{d}{dt}\|\mathbf{u}\|^2 + \mathrm{Re}^{-1} \|\nabla \mathbf{u}\|^2 + \chi \int_\Omega (\mathbf{u} - \bar{\mathbf{u}})\mathbf{u}\, d\Omega = 0.$$

Integrating in time, we obtain

$$\frac{1}{2}\|\mathbf{u}(T)\|^2 + \int_0^T \mathrm{Re}^{-1} \|\nabla \mathbf{u}\|^2\, dt + \int_0^T \chi \int_\Omega (\mathbf{u} - \bar{\mathbf{u}})\mathbf{u}\, d\Omega\, dt = \frac{1}{2}\|\mathbf{u}(0)\|^2. \tag{4.4}$$

Based on equation (4.4), we conclude that the TRM has the same energy as the NSE, but an extra dissipation ϵ_{TRM}, [25], defined as

$$\epsilon_{TRM} = \int_0^T \mathrm{Re}^{-1} \|\Delta \mathbf{u}\|^2\, dt + \int_0^T \chi \int_\Omega (\mathbf{u} - \bar{\mathbf{u}})\mathbf{u}\, d\Omega\, dt. \tag{4.5}$$

We want to understand what happens to the energy of a fluid that is driven by this time relaxation model. If there are some changes in the partial differential equations, there will be a change in energy as well. The additional energy dissipation in the time relaxation model by $\chi(\mathbf{u} - \bar{\mathbf{u}})$ causes the energy to dissipate faster, [27].

It is important to show that the extra dissipation integral is nonnegative, i.e.

$$\int_0^T \chi \int_\Omega (\mathbf{u} - \bar{\mathbf{u}})\mathbf{u}\, d\Omega\, dt \geq 0$$

because if it is negative the energy balance makes no sense. When a fluid is more viscous (i.e., Re small), the velocity slows down and the energy is lower, [27].

Take the partial differential equation (4.3)

$$-\delta^2 \Delta \bar{\mathbf{u}} + \bar{\mathbf{u}} = \mathbf{u}.$$

Subtracting $\bar{\mathbf{u}}$ from both sides,

$$-\delta^2 \Delta \bar{\mathbf{u}} = \mathbf{u} - \bar{\mathbf{u}}. \tag{4.6}$$

Note that for some ϕ such that

$$-\delta^2 \Delta \bar{\phi} + \bar{\phi} = \phi,$$

we have

$$(-\delta^2 \Delta + \mathbf{I})\bar{\phi} = \phi,$$

which becomes

$$\bar{\phi} = (-\delta^2 \Delta + \mathbf{I})^{-1} \phi,$$

where

$$(-\delta^2 \Delta + \mathbf{I})^{-1} =: \mathrm{G}.$$

Thus

$$\bar{\phi} = \mathrm{G}(\phi). \tag{4.7}$$

An operator $\mathrm{F} : X \to Y$ is **symmetric positive semi-definite** if

$$(\mathrm{F}u, u) \geq 0 \quad \forall u \neq 0 \text{ in } X.$$

Since G defined in equation (4.7) satisfies this definition, it is symmetric positive semi-definite, [14].

Multiplying by $\mathbf{u}$ and integrating the left hand side of the PDE (4.6) along Ω, and assuming $\mathbf{f} = \mathbf{0}$ along the boundary, we have

$$\begin{aligned}
\int_\Omega (\mathbf{u} - \bar{\mathbf{u}})\mathbf{u}\, d\Omega &= \int_\Omega -\delta^2 \Delta \bar{\mathbf{u}} \cdot \mathbf{u}\, d\Omega, \\
&= \int_\Omega \delta^2 \nabla \bar{\mathbf{u}} \cdot \nabla \mathbf{u}\, d\Omega - \int_\sigma \delta^2 \bar{\mathbf{u}} \cdot \mathbf{n} \cdot \mathbf{u} d\sigma, \\
&= \delta^2 \int_\Omega \nabla \bar{\mathbf{u}} \cdot \nabla \mathbf{u}\, d\Omega, \\
&= \delta^2 \int_\Omega \mathrm{G}(\nabla \mathbf{u}) \cdot \nabla \mathbf{u}\, d\Omega, \\
&= \delta^2 (\mathrm{G}(\nabla \mathbf{u}), \nabla \mathbf{u}) \geq 0,
\end{aligned}$$

since G is symmetric positive semi-definite. Thus

$$\int_\Omega (\mathbf{u} - \bar{\mathbf{u}}) \cdot \mathbf{u}\, d\Omega \geq 0,$$

so

$$\int_0^T \chi \int_\Omega (\mathbf{u} - \bar{\mathbf{u}}) \cdot \mathbf{u}\, d\Omega\, dt \geq 0.$$

Enstrophy Balance for the Time Relaxation Model

Take the same system of partial differential equations (4.1)–(4.3) and assume no body force $\mathbf{f} = \mathbf{0}$ and $\nu = 0$. The enstrophy remains the same in the absence of body force and viscosity, and the system changes if $\mathbf{f} \neq \mathbf{0}$ and/or $\nu \neq 0$, [27].

Multiplying (4.1) by $\Delta\mathbf{u}$, and integrating in space and time, letting $\sigma = \partial\Omega$, we obtain

$$\int_\Omega \mathbf{u}_t \cdot \Delta\mathbf{u}\, d\Omega + \int_\Omega \mathbf{u} \cdot \nabla\mathbf{u} \cdot \Delta\mathbf{u}\, d\Omega - \int_\Omega \mathrm{Re}^{-1}\Delta\mathbf{u} \cdot \Delta\mathbf{u}\, d\Omega + \int_\Omega \nabla p \cdot \Delta\mathbf{u}\, d\Omega + \int_\Omega \chi(\mathbf{u} - \bar{\mathbf{u}}) \cdot \Delta\mathbf{u}\, d\Omega = 0,$$

where

$$\begin{aligned}\int_\Omega \mathbf{u}_t \cdot \Delta\mathbf{u}\, d\Omega &= -\int_\Omega (\nabla \times \mathbf{u}_t) \cdot (\nabla \times \mathbf{u}\, d\Omega) + \int_\sigma \mathbf{u}_t \cdot \nabla \times \mathbf{u} \cdot \mathbf{n} d\sigma, \\ &= -\int_\Omega (\nabla \times \mathbf{u}_t) \cdot (\nabla \times \mathbf{u})\, d\Omega, \\ &= -\frac{1}{2}\frac{d}{dt} \|\nabla \times \mathbf{u}\|^2,\end{aligned}$$

and

$$\begin{aligned}&\int_\Omega \mathbf{u} \cdot \nabla\mathbf{u} \cdot \Delta\mathbf{u}\, d\Omega = 0, \\ &-\int_\Omega \mathrm{Re}^{-1}\Delta\mathbf{u} \cdot \Delta\mathbf{u}\, d\Omega = -\mathrm{Re}^{-1}\int_\Omega \Delta\mathbf{u} \cdot \Delta\mathbf{u}\, d\Omega = -\mathrm{Re}^{-1}\|\Delta\mathbf{u}\|^2, \\ &\int_\Omega \nabla p \cdot \Delta\mathbf{u}\, d\Omega = -\int_\Omega (\nabla \times \nabla p) \cdot (\nabla \times \mathbf{u})\, d\Omega = 0,\end{aligned}$$

since the curl of a gradient is zero.

$$\chi \int_\Omega (\mathbf{u} - \bar{\mathbf{u}}) \Delta \mathbf{u} \, d\Omega = \chi \int_\Omega -\delta^2 \Delta \bar{\mathbf{u}} \cdot \Delta \mathbf{u} \, d\Omega.$$

Moreover,

$$\chi \delta^2 \int_\Omega \Delta \bar{\mathbf{u}} \cdot \Delta \mathbf{u} \, d\Omega = -\chi \delta^2 (\mathrm{G}(\Delta \mathbf{u}), \Delta \mathbf{u}),$$

where $(\mathrm{G}(\Delta \mathbf{u}), \Delta \mathbf{u}) \geq 0$ since G is symmetric positive semi-definite. This gives

$$-\frac{1}{2} \frac{d}{dt} \left\| \nabla \times \mathbf{u} \right\|^2 - \mathrm{Re}^{-1} \left\| \Delta \mathbf{u} \right\|^2 - \chi \delta^2 \int_\Omega \Delta \bar{\mathbf{u}} \cdot \Delta \mathbf{u} \, d\Omega = 0.$$

Mutliplying by -1,

$$\frac{1}{2} \frac{d}{dt} \left\| \nabla \times \mathbf{u} \right\|^2 + \mathrm{Re}^{-1} \left\| \Delta \mathbf{u} \right\|^2 + \chi \delta^2 \int_\Omega \Delta \bar{\mathbf{u}} \cdot \Delta \mathbf{u} \, d\Omega = 0.$$

Integrating with respect to time t, we have

$$\begin{aligned} \frac{1}{2} \left\| \nabla \times \mathbf{u}(T) \right\|^2 + \int_0^T \mathrm{Re}^{-1} \left\| \Delta \mathbf{u} \right\|^2 \, dt \\ + \int_0^T \chi \delta^2 \int_\Omega \Delta \bar{\mathbf{u}} \cdot \Delta \mathbf{u} \, d\Omega \, dt = \frac{1}{2} \left\| \nabla \times \mathbf{u}(0) \right\|^2. \end{aligned} \tag{4.8}$$

As with the energy, we conclude that the TRM has the same enstrophy as the NSE, but an enhanced dissipaton ε_{TRM}, defined as

$$\varepsilon_{TRM} = \int_0^T \mathrm{Re}^{-1} \left\| \Delta \mathbf{u} \right\|^2 dt + \int_0^T \chi \delta^2 \int_\Omega \Delta \bar{\mathbf{u}} \cdot \Delta \mathbf{u} \, d\Omega \, dt. \tag{4.9}$$

Note that when $\chi = 0$ and/or $\delta = 0$, this integral is 0, and we are back to the NSE. Thus, the enstrophy balance will be the same as the standard one for the NSE. This is the same for both the energy and enstrophy balances, [27].

CHAPTER 5

NUMERICAL ANALYSIS OF THE TIME RELAXATION MODEL

Herein, we introduce the finite element method, derive the finite element variational formulation for the TRM and use it to simulate a flow for a specific benchmark problem.

Introduction

In the study of more difficult fluid flows, certain numerical methods are needed to solve the model's equations, [29]. Numerical methods are methods for solving problems in terms of numbers or graphical representations. In the study of numerical methods, the range of applicability and the accuracy of the methods are investigated and considered, [23].

In numerical methods, the steps from a given situation to a conclusion include setting up a mathematical model of the problem, choosing an appropriate method, programming into a computer algebra system, doing the computation, and interpreting the results. As such, algorithms are very important in the formulation of numerical methods. Algorithms are written in a step-by-step procedure that states the method in a form understandable to humans, and they are then used to write a program to execute the method in a language the computer can understand, [23].

Finite Element Method

An important numerical method with respect to the Navier-Stokes Equations is the finite element method. The finite element method states that the solution u of a differential equation can be represented as a linear combination of unknown parameters c_j and selected functions ϕ_j. The parameters c_j are chosen so that the differential equation is satisfied, and the functions ϕ_j, called *approximation functions* are selected such that the satisfy the boundary conditions of the problem, [20].

In applications, regions are geometrically complex, making it difficult to generate approximate functions that satisfy the different boundary conditions on different portions of the boundary. In the finite element method, the given domain is viewed as a collection subdomains, called *finite elements*, where it is possible to generate the given ϕ_j, [20]. These subdomains are simpler geometric shapes, usually triangles or rectangles. We seek the approximate solutions on these subdomains because it is easier to represent the more complicated functions as a collection of simple polynomials. It is important that each segment of the solution "fits" with its neighbors; i.e. the function and its partial derivatives up to a given order are continuous at the connecting points, [30].

The first step in the finite element method is then setting up the domain into this finite set of elements. The subsequent steps include weighted-integral or weak formulation of the differential equation to be analyzed and developing the finite element model for the problem. The finite elements are then assembled to obtain a global system of algebraic equations, and

the boundary conditions are imposed to solve the equation. Finally, the solutions are computed, and the quantities of interest are found, [20].

Weak Formulation of the NSE

Consider the non-dimensional Navier-Stokes Equations (2.3) and (2.4) with no-slip boundary conditions (i.e. $\mathbf{u} = \mathbf{0}$ on $\partial\Omega$):

$$\mathbf{u}_t + \mathbf{u} \cdot \nabla \mathbf{u} - \mathrm{Re}^{-1} \Delta \mathbf{u} + \nabla p = \mathbf{f},$$

$$\nabla \cdot \mathbf{u} = 0.$$

Also consider the space $L^2(\Omega)$ with inner product $(\mathbf{u}, \mathbf{v}) = \int_\Omega \mathbf{u} \cdot \mathbf{v}$. Also consider the Sobolev space $W^{m,p}(\Omega)$, defined as the set of all functions $u \in L^p(\Omega)$ such that $D^\alpha u \in L^p(\Omega)$ for all $|\alpha| \leq m$; that is, all derivatives up to a given order are in the space $L^p(\Omega)$. When $p = 2$, the Sobolev space is an inner product space, and a subspace of $L^2(\Omega)$. We write $H_0^1(\Omega)$ or $H^1(\Omega)$ instead of $W^{k,2}(\Omega)$, [14].

Let the velocity space X be defined as

$$\text{Velocity Space—} X := H_0^1(\Omega).$$

Also, define the pressure space

$$\text{Pressure Space—}P := L_0^2(\Omega) = \left\{ q \in L^2(\Omega) : \int_\Omega q \, d\Omega = 0 \right\}.$$

From the divergence-free condition $\nabla \cdot \mathbf{u} = 0$, define the divergence-free space as

$$\text{Divergence-free Space—}Z := \left\{ v \in X : \int_\Omega q \, \nabla \cdot \mathbf{v} \, d\Omega = 0, \ \forall q \in P \right\}.$$

Also denote the dual space of X as X', with norm $\|\cdot\|_{-1}$,[28].

Multiplying (2.3) by a test function $\mathbf{v} \in X, q \in P$ and integrating over Ω, we have

$$(\mathbf{u}_t, \mathbf{v}) + (\mathbf{u} \cdot \nabla \mathbf{u}, \mathbf{v}) - \mathrm{Re}^{-1} (\Delta \mathbf{u}, \mathbf{v}) + (\nabla p, \mathbf{v}) = (\mathbf{f}, \mathbf{v}) \quad \forall \mathbf{v} \in X;$$

$$(\nabla \cdot \mathbf{u}, q) = 0 \quad \forall q \in P.$$

Take, by Green's formula,

$$(\Delta \mathbf{u}, \mathbf{v}) = \int_X (\Delta \mathbf{u}) \cdot \mathbf{v} \, dX = \int_G \mathbf{v} \nabla \mathbf{u} \cdot \mathbf{n} \, dG - \int_X \nabla \mathbf{u} \cdot \nabla \mathbf{v} \, dX,$$

where $G = \partial X$. Since the velocity space X has homogeneous boundary conditions, we have $\int_G \mathbf{v} \nabla \mathbf{u} \cdot \mathbf{n} \, dG = 0$. Therefore,

$$(\Delta \mathbf{u}, \mathbf{v}) = - \int_X \nabla \mathbf{u} \cdot \nabla \mathbf{v} \, dX = - (\nabla \mathbf{u}, \nabla \mathbf{v}).$$

By the divergence theorem, we get

$$(\nabla p, \mathbf{v}) = \int_X (\nabla p)\, \mathbf{v}\, dX = \int_G p \cdot \mathbf{v} \cdot \mathbf{n}\, dG - \int_X p \nabla \cdot \mathbf{v}\, dX,$$

where $\int_G p \cdot \mathbf{v} \cdot \mathbf{n}\, dG = 0$ by the boundary conditions. Then

$$(\nabla p, \mathbf{v}) = -\int_X p \cdot (\nabla \cdot \mathbf{v})\ dX = -(p, \nabla \cdot \mathbf{v}).$$

Also,

$$(\nabla \cdot \mathbf{u}, q) = \int_X (\nabla \cdot \mathbf{u})\, q\, dX = 0,$$

by the divergence-free space. Thus, the weak formulation for the NSE can be stated as follows: *Find* $(\mathbf{u}, p) \in X \times P$ *satisfying:*

$$(\mathbf{u}_t, \mathbf{v}) + (\mathbf{u} \cdot \nabla u, \mathbf{v}) - (p, \nabla \cdot \mathbf{v}) + \mathrm{Re}^{-1} (\nabla \mathbf{u}, \nabla \mathbf{v}) = (\mathbf{f}, \mathbf{v}) \quad \forall \mathbf{v} \in X; \tag{5.1}$$

$$(q, \nabla \cdot \mathbf{u}) = 0 \quad \forall q \in P; \tag{5.2}$$

$$\mathbf{u}(0, \mathbf{x}) = \mathbf{u}_0(\mathbf{x}) \quad \forall \mathbf{x} \in \Omega. \tag{5.3}$$

Next, we look at the filtering. Let $\phi \in L^2(\Omega)$ and $\delta > 0$, and let $\overline{\phi}$ be the result of a filtering operation on ϕ, [28]. Then, as in (4.3), $\overline{\phi}$ is the unique solution of

$$-\delta^2 \Delta \overline{\phi} + \overline{\phi} = \phi,$$

where

$$\left(\mathbf{I}-\delta^2\Delta\right)\overline{\phi}=\phi,$$

$$\overline{\phi}=\left(\mathbf{I}-\delta^2\Delta\right)^{-1}\phi,$$

$$\overline{\phi}=G(\phi),$$

for an operator $G=\left(\mathbf{I}-\delta^2\Delta\right)^{-1}\phi$, where G is symmetric positive semi-definite, [14], [28]. Then from [28], we have the following notation:

$$\|\phi^*\|=\left(\phi-G(\phi),\phi\right)^{1/2}. \tag{5.4}$$

Using the same process as for the NSE, we can define the weak formulation for the TRM, which can be stated as follows: *Find* $(\mathbf{u},p)\in X\times P$ *satisfying:*

$$\begin{aligned}\left(\mathbf{u}_t,\mathbf{v}\right)+\left(\mathbf{u}\cdot\nabla\mathbf{u},\mathbf{v}\right)-\left(p,\nabla\cdot\mathbf{v}\right)+\mathrm{Re}^{-1}\left(\nabla\mathbf{u},\nabla\mathbf{v}\right)+\\ \chi\left(\mathbf{u}-\bar{\mathbf{u}},\mathbf{v}\right)=\left(\mathbf{f},\mathbf{v}\right),\quad\forall\mathbf{v}\in X,\end{aligned} \tag{5.5}$$

$$\left(q,\nabla\cdot\mathbf{u}\right)=0,\quad\forall q\in P. \tag{5.6}$$

In order to solve equations (5.5)–(5.6) by the finite element method, we must construct finite dimensional subspaces X_h,Q_h,Z_h of our velocity, pressure, and divergence-free spaces, respectively, with piecewise continuous test functions, [7]. Let $\Omega\subset\mathbb{R}^d\,(d=2,3)$ be a polygonal domain and let T_h be a triangulation of Ω consisting of either triangles (in the 2D

case) or tetrahedrals (in the 3D case), [7], [28]. Also, let $\bar{\Omega}$ be the closure of Ω. Then

$$\Omega = \bigcup_{K \in T_h} K.$$

Let $P_k(K)$ be the space of polynomials on K of degree less than or equal to K. Since test functions $\mathbf{v} \in P_k(K), q \in P_s(K)$ must be continuous at all internal vertices of the subdomain, we have $\mathbf{v} \in C(\bar{\Omega})^d \, (d = 2, 3), q \in C(\bar{\Omega})$. Then the finite element spaces are defined as

$$\begin{aligned} X_h &:= \left\{ \mathbf{v} \in X \cap C\left(\bar{\Omega}\right)^d : \mathbf{v}|_k \in P_k(K), \ , \forall K \in T_h \right\}; \\ P_h &:= \left\{ q \in P \cap C\left(\bar{\Omega}\right) : \mathbf{v}|_k \in P_s(K), \ , \forall K \in T_h \right\}; \\ Z_h &:= \left\{ \mathbf{v} \in X_h : (q, \nabla \cdot \mathbf{v}) = 0, \ \forall q \in P_h \right\}. \end{aligned}$$

Assume that the spaces X_h, P_h satisfy the following compatibility condition, known as the *discrete inf-sup condition*, [7], [17]: there exists $\gamma \in \mathbb{R}, \gamma > 0$,

$$\gamma \leq \inf_{q_h \in P_h} \sup_{\mathbf{v}_h \in X_h} \frac{\int_\Omega q_h \nabla \cdot \mathbf{v}_h dA}{\|q_h\|_P \|\mathbf{v}_h\|_X}. \tag{5.7}$$

As in [28], define the *skew-symmetric trilinear form* $b^*(\cdot, \cdot, \cdot) : X \times X \times X \to \mathbb{R}$ as

$$b^*(\mathbf{u}, \mathbf{v}, \mathbf{w}) := \frac{1}{2} (\mathbf{u} \cdot \nabla \mathbf{v}, \mathbf{w}) - \frac{1}{2} (\mathbf{u} \cdot \nabla \mathbf{w}, \mathbf{v}).$$

For $\mathbf{u}, \mathbf{v}, \mathbf{w} \in X$, with $\nabla \cdot \mathbf{u} = 0$,

$$b^*(\mathbf{u}, \mathbf{v}, \mathbf{w}) := (\mathbf{u} \cdot \nabla \mathbf{v}, \mathbf{w}).$$

We define the *discrete differential filter*, where $\overline{\phi}^h \in X_h$ is the unique solution of

$$\delta^2 \left(\nabla \overline{\phi}^h, \nabla \mathbf{v}_h \right) + \left(\overline{\phi}^h, \mathbf{v}_h \right) = \left(\phi, \mathbf{v}_h \right), \quad \forall \mathbf{v}_h \in X_h. \tag{5.8}$$

For internal flows under no-slip boundary conditions, incompressibility must be preserved. In this case, the *Stokes differential filter*, based upon the Stokes' equations, is used, [28]. Here, $\left(\overline{\phi}^h, p \right) \in X_h \times P_h$ is the unique solution of

$$\delta^2 \left(\nabla \overline{\phi}^h, \nabla \mathbf{v}_h \right) + \left(\overline{\phi}^h, \mathbf{v}_h \right) - \left(p, \nabla \cdot \mathbf{v}_h \right) = \left(\phi, \mathbf{v}_h \right), \quad \forall \mathbf{v}_h \in X_h, \tag{5.9}$$

$$\left(\nabla \cdot \overline{\phi}^h, q \right) = 0, \quad \forall q \in P_h. \tag{5.10}$$

We use a Crank-Nicholson scheme on (5.5)–(5.6). Let $\mathbf{u}_t \approx \frac{\mathbf{u}_h^{n+1} - \mathbf{u}_h^n}{\Delta t}$ and $\mathbf{u}\left(t^{n+1/2}\right) = \mathbf{u}^{n+1/2} = \frac{1}{2}\left(\mathbf{u}(t_n) - \mathbf{u}(t_{n-1})\right)$. From the weak formulation of the TRM and definition of trilinear form, the finite element formulation for the TRM can be stated as follows: *Find* $(\mathbf{u}_h, p_h) \in X_h \times P_h$ *such that*

$$\begin{aligned} &\frac{1}{\Delta t}\left(\mathbf{u}_h^{n+1} - \mathbf{u}_h^n, \mathbf{v}_h \right) + b^*\left(\mathbf{u}_h^{n+1/2}, \mathbf{u}_h^{n+1/2}, \mathbf{v}_h \right) + \mathrm{Re}^{-1}\left(\nabla \mathbf{u}_h^{n+1/2}, \nabla \mathbf{v}_h \right) \\ &- \left(p_h^{n+1/2}, \nabla \cdot \mathbf{v}_h \right) + \chi\left(\mathbf{u}_h^{n+1/2} - \overline{\mathbf{u}_h^{n+1/2}}^h, \mathbf{v}_h \right) = \left(\mathbf{f}\left(t^{n+1/2}\right), \mathbf{v}_h \right), \quad \forall \mathbf{v}_h \in X_h, \end{aligned} \tag{5.11}$$

$$\left(q_h, \nabla \cdot \mathbf{u}_h^{n+1} \right) = 0, \quad \forall q_h \in P_h. \tag{5.12}$$

Because the spaces X_h, P_h satisfy the discrete inf-sup condition, (5.11)-(5.12) are equivalent to the following problem, [28]:

For $n = 1, 2, \ldots, M-1$ find $\mathbf{u}_h^{n+1} \in Z_h$ such that

$$\begin{aligned} \frac{1}{\Delta t}\left(\mathbf{u}_h^{n+1} - \mathbf{u}_h^n, \mathbf{v}_h\right) + b^*\left(\mathbf{u}_h^{n+1/2}, \mathbf{u}_h^{n+1/2}, \mathbf{v}_h\right) + \mathrm{Re}^{-1}\left(\nabla \mathbf{u}_h^{n+1/2}, \nabla \mathbf{v}_h\right) \\ +\chi\left(\mathbf{u}_h^{n+1/2} - \overline{\mathbf{u}_h^{n+1/2}}^h, \mathbf{v}_h\right) = \left(\mathbf{f}\left(t^{n+1/2}\right), \mathbf{v}_h\right), \quad \forall \mathbf{v}_h \in X_h; \end{aligned} \tag{5.13}$$

$$\left(q_h, \nabla \cdot \mathbf{u}_h^{n+1}\right) = 0, \quad \forall q_h \in P_h. \tag{5.14}$$

There are many different options for polynomial spaces $(P_k(K), P_s(K))$. One of the simplest is the *Taylor-Hood* element, (P_k, P_{k-1}). That is, test functions $\mathbf{v} \in P_k(K), q \in P_{k-1}(K)$. It would appear that the simplest choice for the numerical solutions of the TRM would be (P_1, P_0), where the test functions for velocity are piecewise linear and constant and the test functions for pressure are piecewise constant. However, this is unsuitable for the Stokes equations, as the velocity space is too small for any meaningful approximations, and the inf-sup condition is not satisfied, [8]. Thus, the lowest order Taylor-Hood element is (P_2, P_1), where velocity test functions are polynomials and pressure functions are piecewise linear continuous functions, [8].

Our final program consists of a nested for loop, with an outer loop for each time iteration, and a fixed point iteration loop for the nonlinear term in the TRM, within each time iteration. Pseudocode for the fixed point iteration loop is given by Algorithm 1.

Stability of the Finite Element Formulation

In the development of the algorithm, it is important to show that it is *stable*. That is, small changes in initial data should cause only small changes in the final results. If small changes

Algorithm 1 Fixed point iteration loop for the TRM

Choose number of time total iterations $iter$, number of fixed point iterations, $fixediter$

FOR $k = 1, 2, \ldots, iter$

Set $u^{k-1} = u^k, p^{k-1} = p^k$

FOR $n = 1, 2, \ldots, fixediter$

Evaluate Stokes differential filter

Evaluate TRM

If $\max \left| \mathbf{u}_{n-1}^k - \mathbf{u}_n^k \right| < \varepsilon$ **STOP**, move to next time step

END

END

in initial data produce large changes in final results, the algorithm is said to be *unstable*, [23]. The corresponding scheme for a time-dependent PDE is said to be stable in a norm $\|\cdot\|$ if, assuming no body force, there exists a constant C such that

$$\|u^n\| \leq C \left\|u^0\right\|,$$

where C is independent of $\Delta t, \Delta x$ and initial condition u^0, [7].

We use the discrete Gronwall's lemma, [17]: Let $\Delta t, H$, and a_n, b_n, c_n, γ_n (for integers $n \geq 0$) be nonnegative numbers such that

$$a_l + \Delta t \sum_{n=0}^{l} \leq \Delta t \sum_{n=0}^{l} \gamma_n a_n + \Delta t \sum_{n=0}^{l} c_n + H \quad \text{for } l \geq 0.$$

Suppose that $\Delta t\gamma_n < 1$, for all n, and set $\sigma_n = (1 - \Delta t\gamma_n)^{-1}$. Then,

$$a_l + \Delta t \sum_{n=0}^{l} b_n \leq \exp\left(\Delta \sum_{n=0}^{l} \sigma_n\gamma_n\right)\left\{\Delta t \sum_{n=0}^{l} c_n + H\right\} \quad \text{for } l \geq 0.$$

We want to show that the scheme has the following a priori bound:

$$\left\|\mathbf{u}_h^l\right\|^2 + 2\Delta t\chi \sum_{n=1}^{l} \|\hat{\mathbf{u}}_h^{n*}\|^2 + 2\Delta t\nu \sum_{n=1}^{l} \|\Delta\hat{\mathbf{u}}_h^n\|^2 \leq C\left(\|f\|_{2,0}^2 + \left\|\mathbf{u}_h^0\right\|^2\right).$$

To show that the scheme (5.11)–(5.12) is stable, let $\mathbf{v}_h = \mathbf{u}_h^{n+\frac{1}{2}}$ in (5.13). Then the trilinear term vanishes, leaving

$$\frac{1}{\Delta t}\left(\mathbf{u}_h^{n+1} - \mathbf{u}_h^n, \mathbf{u}_h^n\right) + \mathrm{Re}^{-1}\left(\nabla\mathbf{u}_h^{n+\frac{1}{2}}, \nabla\mathbf{u}_h^{n+\frac{1}{2}}\right) + \chi\left(\mathbf{u}_h^{n+\frac{1}{2}} - \overline{\mathbf{u}_h^{n+\frac{1}{2}}}^h, \mathbf{u}_h^{n+\frac{1}{2}}\right)$$
$$= \left(\mathbf{f}\left(t^{n+\frac{1}{2}}\right), \mathbf{u}_h^{n+\frac{1}{2}}\right).$$

Then we have

$$\begin{aligned}
\frac{1}{\Delta t}\left(\mathbf{u}_h^{n+1} - \mathbf{u}_h^n, \mathbf{u}_h^n\right) &= \frac{1}{\Delta t}\left(\mathbf{u}_h^{n+1} - \mathbf{u}_h^n, \frac{\mathbf{u}_h^{n+1} + \mathbf{u}_h^n}{2}\right), \\
&= \frac{1}{2\Delta t}\left(\mathbf{u}_h^{n+1} - \mathbf{u}_h^n, \mathbf{u}_h^{n+1} + \mathbf{u}_h^n\right), \\
&= \frac{1}{2\Delta t}\left[\left(\mathbf{u}_h^{n+1}, \mathbf{u}_h^{n+1}\right) + \left(\mathbf{u}_h^{n+1}, \mathbf{u}_h^n\right) - \left(\mathbf{u}_h^{n+1}, \mathbf{u}_h^n\right) - \left(\mathbf{u}_h^n, \mathbf{u}_h^n\right)\right], \\
&= \frac{1}{2\Delta t}\left[\left\|\mathbf{u}_h^{n+1}\right\|^2 - \|\mathbf{u}_h^n\|^2\right].
\end{aligned}$$

Similarly, we have

$$\mathrm{Re}^{-1}\left(\nabla\mathbf{u}_h^{n+\frac{1}{2}}, \nabla\mathbf{u}_h^{n+\frac{1}{2}}\right) = \mathrm{Re}^{-1}\left\|\nabla\mathbf{u}_h^{n+\frac{1}{2}}\right\|^2.$$

By equation (5.4),

$$\chi\left(\mathbf{u}_h^{n+\frac{1}{2}}-\overline{\mathbf{u}_h^{n+\frac{1}{2}}}^h,\mathbf{u}_h^{n+\frac{1}{2}}\right)=\chi\left(\mathbf{u}_h^{n+\frac{1}{2}}-G^h\left(\mathbf{u}_h^{n+\frac{1}{2}}\right),\mathbf{u}_h^{n+\frac{1}{2}}\right)=\chi\left\|\mathbf{u}_h^{n+\frac{1}{2}^*}\right\|^2.$$

By the Cauchy-Schwarz and Young's inequalities,

$$\left(\mathbf{f}\left(t^{n+\frac{1}{2}}\right),\mathbf{u}_h^{n+\frac{1}{2}}\right)\leq\frac{\mathrm{Re}}{2}\left\|\mathbf{f}\left(t^{n+\frac{1}{2}}\right)\right\|_{-1}^2+\frac{\mathrm{Re}^{-1}}{2}\left\|\nabla\mathbf{u}_h^{n+\frac{1}{2}}\right\|^2.$$

So we have

$$\frac{1}{2\Delta t}\left[\left\|\mathbf{u}_h^{n+1}\right\|^2-\left\|\mathbf{u}_h^n\right\|^2\right]+\frac{\mathrm{Re}^{-1}}{2}\left\|\nabla\mathbf{u}_h^{n+\frac{1}{2}}\right\|^2+\chi\left\|\mathbf{u}_h^{n+\frac{1}{2}^*}\right\|^2\leq\frac{\mathrm{Re}}{2}\left\|\mathbf{f}\left(t^{n+\frac{1}{2}}\right)\right\|_{-1}^2.$$

Summing from $n=1$ to $M-1$ gives

$$\frac{1}{2\Delta t}\left[\left\|\mathbf{u}_h^M\right\|^2-\left\|\mathbf{u}_h^0\right\|^2\right]+\chi\sum_{n=1}^{M-1}\left\|\mathbf{u}_h^{n+\frac{1}{2}^*}\right\|^2+\mathrm{Re}^{-1}\sum_{n=1}^{M-1}\left\|\mathbf{u}_h^{n+\frac{1}{2}}\right\|^2\leq\sum_{n=1}^{M-1}\left\|\mathbf{f}^{n+\frac{1}{2}}\right\|_{-1}^2,$$

which becomes

$$\begin{aligned}\left\|\mathbf{u}_h^M\right\|^2+2\Delta t\chi\sum_{n=1}^{M-1}\left\|\mathbf{u}_h^{n+\frac{1}{2}^*}\right\|^2+\Delta t\mathrm{Re}^{-1}\sum_{n=1}^{M-1}\left\|\mathbf{u}_h^{n+\frac{1}{2}}\right\|^2\\ \leq\left\|\mathbf{u}_h^0\right\|^2+\Delta t\mathrm{Re}\sum_{n=1}^{M-1}\left\|\mathbf{f}^{n+\frac{1}{2}}\right\|_{-1}^2.\end{aligned}$$

By the discrete Gronwall's lemma, we have our unconditional stability result, [17].

CHAPTER 6

NUMERICAL EXAMPLE: TAYLOR-GREEN VORTEX

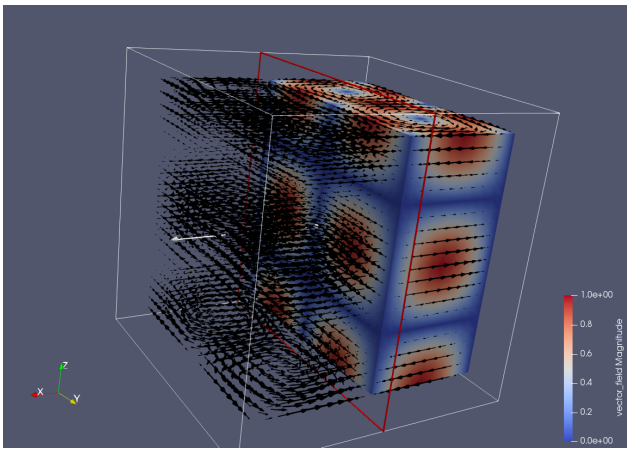

Figure 6.1: A three-dimensional representation of the initial Taylor-Green vortex over the domain $[0, 2\pi]^3$. The domain is represented in two "slices": one to show the velocity vectors and one to show the surfaces and velocity contours.

The Taylor-Green vortex is an unsteady flow of a decaying vortex, with an exact closed form solution of the incompressible NSE, [4], [5]. Solution of the Taylor-Green vortex are among the few known analytical solutions to the NSE, and they are often used as a benchmark to test the accuracy of algorithms solving the NSE, [4]. It is a three-dimensional,

incompressible flow that evolves from a two-dimensional velocity field, [17], given by

$$u_1(x, y, z, 0) = \sin(x)\cos(y)\cos(z),$$

$$u_2(x, y, z, 0) = -\cos(x)\sin(y)\cos(z),$$

$$u_3(x, y, z, 0) = 0,$$

and periodic boundary conditions on $[0, 2\pi]^3$, [15], [18].

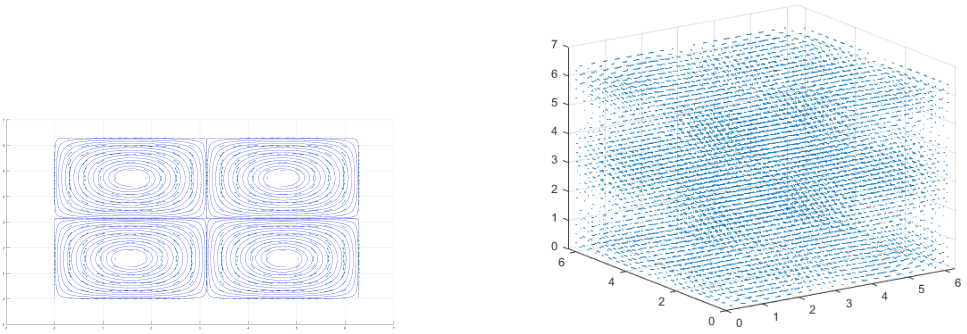

(a) The two-dimensional velocity field for the Taylor-Green vortex.

(b) The three-dimensional flow of the Taylor-Green vortex

Figure 6.2: The Taylor-Green vortex.

Figure 6.2 shows the initial velocity of the Taylor-Green vortex for the domain $[0, 2\pi]^3$. Taking a cross-section of the xy-plane at $z = 0$, figure 6.2a shows the two-dimensional velocity field, consisting of flows moving to the center of four individual vortices. The vortices in the top left and bottom right of the xy-plane move in the counterclockwise direction, while the two vortices in the top right and bottom left move in the clockwise direction. The three-dimensional flow is shown by figure 6.2b.

Let the initial density $\rho(\mathbf{x}, 0) = 1$, [15]. The initial kinetic energy is

$$\begin{aligned} K(0) &= \int_0^{2\pi}\int_0^{2\pi}\int_0^{2\pi} \frac{\rho(\mathbf{x},\mathbf{0})\cdot\mathbf{u_1}(\mathbf{x},\mathbf{0})\cdot\mathbf{u_1}(\mathbf{x},\mathbf{0})}{2} dxdydz, \\ &= \frac{1}{4}\int_0^{2\pi}\int_0^{2\pi}\int_0^{2\pi} [1-\cos(2x)\cos(2y)]\cos^2(z) dxdydz, \\ &= \pi^3, \end{aligned}$$

and is conserved for the Taylor-Green vortex. Therefore, numerical dissipation in a given algorithm can be examined by observing the rate of decrease of the kinetic energy from its initial value π^3 over time, [15], [18]. For the Taylor-Green vortex, the flow develops a singularity at the center of a highly twisted vortex core, and the production of vorticity and enstrophy is proportional to the derivative of the velocity vector. Thus, there should be a growth in enstrophy seen in the simulation results, [18]. Figure 6.3 shows the vorticity of the Taylor-Green vortex at initial time. Vorticity vectors are given in red. Using the right-hand rule, we see that the vorticity is positive for the two vortices moving in the counterclockwise direction. Conversely, vorticity is negative for the two vortices moving the clockwise direction.

We show the effects of the time relaxation model at two different mesh sizes: a course mesh consisting of 6,000 tetrahedral elements, or 10 subintervals in all three directions, and a finer mesh consisting of 16,464 tetrahedral elements, or 14 subintervals in all tree directions. We used the time step $\Delta t = 0.001$ and 100 time steps yielding the time interval $t = [0, 0.1]$.

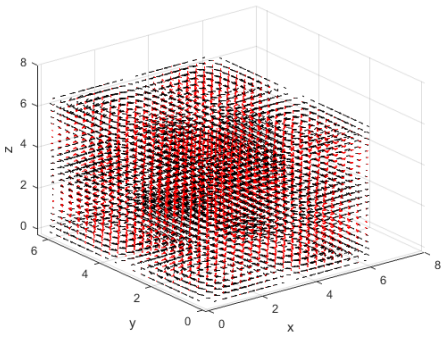

(a) The vorticity (in red) and velocity (in black) of the Taylor-Green vortex in three dimensions

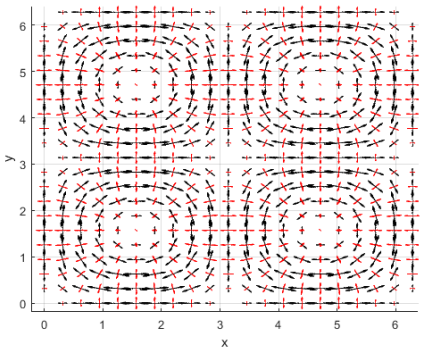

(b) The vorticity (in red) and velocity (in black) field of the Taylor-Green vortex, taken along the xy-plane at $z = 0$.

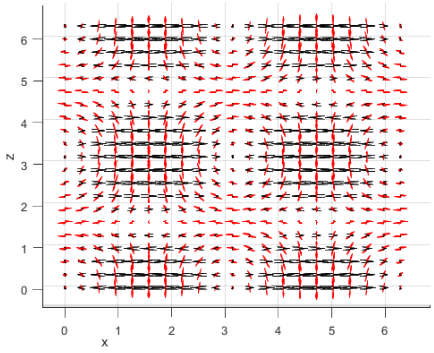

(c) The vorticity (in red) and velocity (in black) field of the Taylor-Green vortex, taken along the xz-plane at $y = 0$.

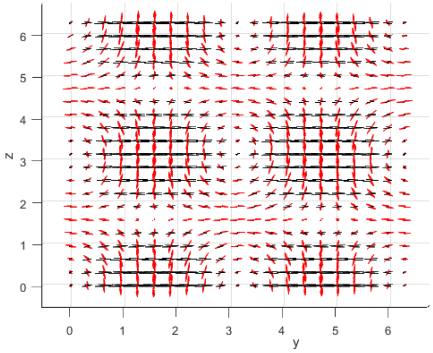

(d) The vorticity (in red) and velocity (in black) field of the Taylor-Green vortex, taken along the yz-plane at $x = 0$.

Figure 6.3: The vorticity of Taylor-Green vortex.

We test the TRM at relaxation parameters $\chi = 0$ (equivalent to the NSE) and $\chi = \Delta t$ at Reynolds number Re = 500,000, using a stop criterion of $\varepsilon = 1 \times 10^{-10}$ for the fixed point iteration loop for the nonlinear term. Using (P_2, P_1) Taylor-Hood elements, we use piecewise quadratic equations for our test functions for velocity and piecewise linear continuous test functions for pressure.

We first considered the coarse mesh of 6,000 tetrahedral elements for $\chi = 0$. The program broke at time $t = 0.046$, failing to meet the stop criterion after only 46 time steps. We next

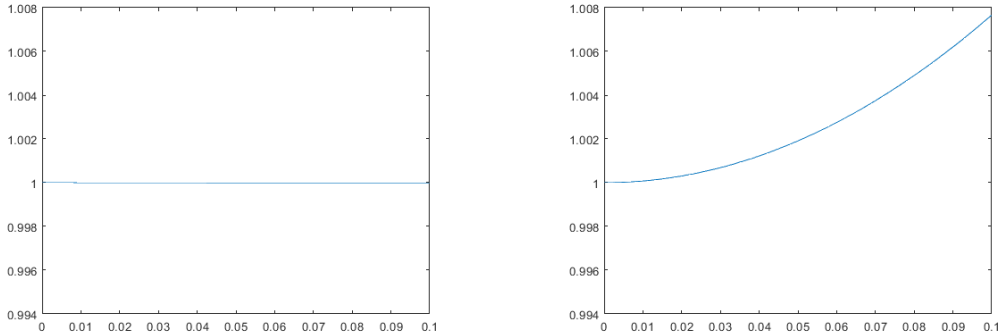

(a) Normalized kinetic energy (b) Normalized enstrophy

Figure 6.4: Energy and enstrophy versus time for Reynolds number Re =500,000 and relaxation parameter $\chi = \Delta t$ for 6,000 tetrahedral elements.

considered the coarse mesh for relaxation parameter $\chi = \Delta t$. In this case, the program ran for the complete time interval, showing the advantages of time relaxation on such a coarse mesh. Figure 6.4 shows the normalized kinetic energy $K(t)/K(0)$ and enstrophy. We see that the enstrophy increases as expected, and the normalized kinetic energy stays constant at near unity.

For the more fine mesh of 16,464 tetrahedral elements, the program was indeed successful for relaxation parameter $\chi = 0$, and the results are given by figure 6.5. It is important to note, however, the increased computational requirement for the standard NSE compared to the TRM in our example. The case of $\chi = 0$ failed on the more coarse mesh of 6,000 tetrahedral elements, the largest mesh size a standard computer with 8GB of RAM can handle. The finer mesh of 16,464 tetrahedral elements required a computer of at least 32 GB of RAM to run smoothly for the complete time interval. It also required significantly more time to run, taking several days to complete all 100 time steps.

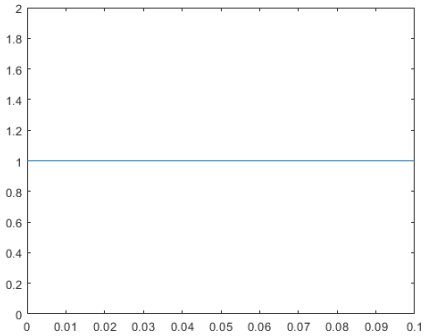

(a) Normalized kinetic energy

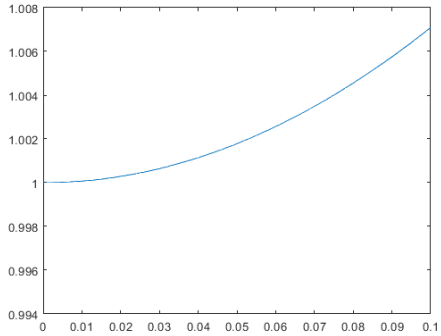

(b) Normalized enstrophy

Figure 6.5: Energy and enstrophy versus time for Reynolds number Re =500,000 and relaxation parameter for 16,464 tetrahedral elements.

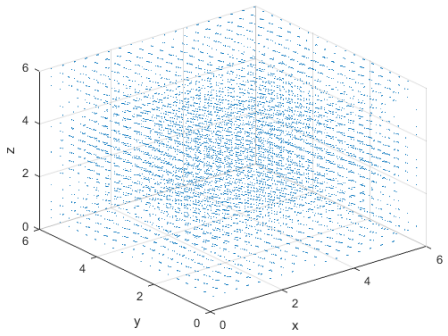

(a) The velocity vectors of the TRM at time $t = 0.1$.

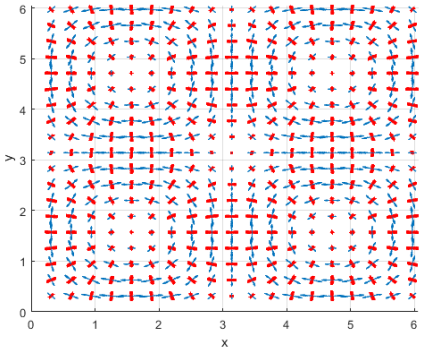

(b) The vorticity (in red) and velocity (in blue) vectors for the TRM at time $t = 0.1$, taken along the xy-plane at $z = 0$.

Figure 6.6: The velocity and vorticity of the TRM.

Figure 6.6 shows the similarities between the velocity and vorticity of the Taylor-Green Vortex and the values of the TRM with $\chi = \Delta t$ at time $t = 0.1$. We observe that the velocity field and vorticity vectors are similar to those of the analytical initial Taylor-Green vortex given by figure 6.3, showing the accuracy of the scheme.

CHAPTER 7

CONCLUSION

We see that in the study of the Navier-Stokes equations, careful consideration must be taken in determining parameters. By non-dimensionalizing the equations, the NSE can be studied in a more general form, with various dimensionless parameters, such as the Reynolds number and the Froude number. These parameters can be adjusted to study their influence on the problem.

Due to the complexities that arise in numerically solving the NSE, the Time Relaxation Model was presented to ease the computational burden, allowing solutions to be found at more coarse mesh sizes than could be used with the standard NSE. Through careful derivation, we have shown that the TRM has the same energy and enstrophy as the NSE but with enhanced dissipation.

Using the finite element method, a finite element formulation was presented for the TRM, which was used as an algorithm for the numerical solution. By using the Taylor-Green vortex, we tested the accuracy of the algorithm. We saw that the kinetic energy was preserved in time and the enstrophy grew as expected.

BIBLIOGRAPHY

[1] K.J. Bathe, The inf-sup condition and its evaluation for mixed finite element methods, *Computer and Structures*, vol. 79, 243–252, 2001.

[2] F. Boyer, P. Fabrie, *Mathematical Tools for the Study of the Incompressible Navier-Stokes Equations and Related Models*. Heidelberg: Springer, 2012.

[3] Berselli, Luigi C., Traian Iliescu and William J. Layton. *Mathematics of Large Eddy Simulation of Turbulent Flows*. Heidelberg: Springer, 2006.

[4] S. Bhatt, Solution of the Taylor-Green Vortex Problem Using Artifical Compressibility Method in Generalized Curvilinear, Co-ordinates, 2016.

[5] M.E. Brachet, D. Meiron, S. Orszag, B. Nickel, R. Morf, and U. Frisch, The Taylor-Green Vortex and Fully Developed Turbulence, *Journal of Statistical Physics*, Vol. 34, 1049–1063, 1984.

[6] J.A. Brighton, W. Hughes. *Schaum's Outlines: Fluid Dynamics. Third Edition*. New York: McGraw-Hill, 1999.

[7] Y. Chen, J. Li, *Computational Partial Differential Equations Using MATLAB*. Boca Raton, CRC Press, 2008.

[8] L. Chen, Finite Element Methods for Stokes Equations, lecture notes, Computational PDES Math 226, University of California, Irvine, delivered 19 March 2018.

[9] S. Childress, *An Introduction to Theoretical Fluid Dynamics*. New York, American Mathematical Society, 2008.

[10] I. Cherkashin, Nondimensionalization of Incompressible Navier-Stokes Equations for Mantle Convection, University of California, Berkley, 2016.

[11] A. Chorin, J. Marsden. *A Mathematical Introduction to Fluid Mechanics, Third Edition*, Springer-Verlag, New York, 1993.

[12] N. Coleman, A Derivation of the Navier-Stokes Equations, *B.S. Undergraduate Mathematics Exchange* Vol 7, No. 1, 20 – 26 (2010)

[13] P.A. Davidson. *Turbulence: An Introduction to Scientists and Engineers, Second Edition*, Oxford University Press, Oxford, 2015.

[14] L. Debnath, P. Mikusinski, *Introduction of Hilbert Spaces with Applications, Third Edition*. Singapore, Elsevier, 2005.

[15] W. Don, D. Gottlieb, C. Shu, O. Schilling, L. Jameson, Numerical Convergence Study of Nearly-Incompressible, Inviscid Taylor-Green Vertex Flow, *Journal of Scientific Computing*, Vol 4, 1–27, 2005.

[16] A.A. Dunca, M. Neda, Numerical Analysis of a Nonlinear Time Relaxation Model of Fluids, *J. Math Anal. Appl.* 420, 1095–1115 (2014)

[17] V.J. Ervin, W.J. Layton, M. Neda, Numerical Analysis of a Higher Order Time Relaxtion Model of Fluids, *International Journal of Numerical Analysis and Modeling* Vol 4, 648–670, 2007.

[18] V.J. Ervin, W.J. Layton, M. Neda, Numerical Analysis of Filter-Based Stabilization for Evolution Equations, *SIAM Journal on Numerical Analysis*, Vol 50, issue 5, 2307–2335, 2012.

[19] C. Foias, O. Manley, R. Rosa, R. Temam, *Encyclopedia of Mathematics and Its Applications: Navier-Stokes Equations and Turbulence*. Cambridge: Cambridge University Press, 2001.

[20] D.K. Gartling, J.N Reddy. *The Finite Element Method in Heat Transfer and Fluid Dynamics, 2nd Edition*. Boca Raton: CRC Press LLC, 2001.

[21] A. Gibiansky, FLuid Dynamics: The Navier-Stokes Equations, Lecture Notes, accessed March 15, 2019.

[22] M. Goltz, J. Huang, *Analytical Modeling of Solute Transport in Groundwater: Using Models to Understand the Effect of Natural Processes on Contaminant Fate and Transport in Groundwater*, Hoboken: Wiley, 2017.

[23] E. Kreyzig. *Advanced Engineering Mathematics*, 9th Edition. Hoboken: John Wiley & Sons, Inc., 2005.

[24] W. Layton, *Introduction to the Numerical Analysis of Incompressible Viscous Flows*, Society for Industrial and Applied Mathematics, Philadelphia, PA, 2008.

[25] W. Layton, M. Neda, Truncation of Scales by Time Relaxation, *J. Math Anal. Appl.*, 325, 788–807, 2007.

[26] R.L. Mott, *Applied Fluid Mechanics, Fourth Edition*, Macmillan Publishing Company, 1994.

[27] M. Neda, T. Hill, Energy and Enstrophy Investigations in Regularized Navier-Stokes Equations, *VI International Conference of Industrial Engineering and Environmental Protection Proceedings*, 177–182, 2016.

[28] M. Neda, X. Sun, L. Yu, Increasing Accuracy and Efficiency for Regularized Navier-Stokes Equations, *Acta Appl Math*, 118, 2011, 57–79.

[29] S.B. Pope, *Turbulent Flows*. Cambridge: Cambridge University Press, 2000.

[30] J.N. Reddy, *An Introductuon to the Finite Element Method, Second Edition*, College Hill, Texas, McGraw Hill, 1993.

[31] P. Saramito, *Complex Fluids: Modeling and Algorithns*, New York, Springer, 2010.

[32] S. Stolz, N.A. Adams, L. Kleiser, The approximate deconvolution model for LES of compressible flows and its application to shock-turbulent-boundary-layer interaction, *Phys. Fluids* 13 (2001) 2985.

[33] S. Stolz, N.A. Adams, L. Kleiser, An approximate deconvolution model for large eddy simulation with application to wall-bounded flows, *Phys. Fluids* 13 (2001) 997.

[34] G. Tryggvason (2017), *The Equations of Fluid Dynamics*, accessed from https://www3.nd.edu/ gtryggva/CFD-Course/NSEquations.pdf

CURRICULUM VITAE

Graduate College
University of Nevada, Las Vegas

Tahj Hill

E-mail address: tahjhill@gmail.com

Degrees:

Bachelor of Science, Mathematical Sciences, 2013
University of Nevada, Las Vegas

Master of Science, Applied Mathematics, 2019
University of Nevada, Las Vegas

Thesis Title: Numerical Analysis and Fluid Flow Modeling of Incompressible Navier Stokes Equations

Thesis Examination Committee:

Chairperson, Dr. Monika Neda, Ph.D.
Committee Member, Dr. Zhonghai Ding, Ph.D.
Committee Member, Dr. Xin Li, Ph.D.
Graduate Faculty Representative, Dr. Dong-Chan Lee, Ph.D.